Fusion Engineering and Design 170 (2021) 112708

Contents lists available at ScienceDirect

Fusion Engineering and Design

journal homepage: www.elsevier.com/locate/fusengdes

Design uncertainty for a HELIAS 5-B stellarator fusion power plant

Stuart I. Muldrew [*,a], Felix Warmer [b], Jorrit Lion [b], Hanni Lux [a]

[a] Culham Centre for Fusion Energy, UK Atomic Energy Authority, Culham Science Centre, Abingdon, Oxfordshire, OX14 3DB, UK
[b] Max-Planck-Institut für Plasmaphysik, Teilinstitut Greifswald, Wendelsteinstrasse 1, Greifswald D-17491, Germany

ARTICLE INFO

Keywords:
Fusion Reactor
Stellarator
HELIAS 5-B
Uncertainty Quantification
System Studies
PROCESS

ABSTRACT

With a lack of plasma disruptions and current-driven instabilities, stellarators are potentially an attractive option for a fusion power plant. Previous system studies have been performed to optimise a HELIAS (HELIcal-axis Advanced Stellarator) 5-B power plant using the systems code PROCESS, however these have been based around a single design point. In reality there is a lot of uncertainty extrapolating from present day devices and understanding. In this paper we study how this will affect the design by identifying eight uncertainty distributions on the input. We then perform parameter studies and Monte-Carlo based analysis to look at the impact on fusion power and divertor heat load. We find that the two uncertainties that have the largest impact on the fusion power are the helium primary coolant mechanical pumping power and the energy multiplication in the blanket and shield. Eighty-three per cent of our solutions are within a tolerable divertor heat load, however this is additionally influenced by the tungsten impurity levels. In order to stay below the density cut-off limit for Electron Cyclotron Resonance Heating, the confinement time needs to be enhanced relative to the ISS04 scaling relation to produce acceptable performance. By identifying the highest impact design parameters, we are able to highlight that research into the blankets should be prioritised to reduce overall design uncertainty.

1. Introduction

Stellarators offer a number of advantages for a fusion reactor power plant and form part of the European Roadmap to fusion energy [1]. There are a number of stellarator configurations proposed and systems studies have been carried out to explore the parameter space of a Heliotron [2] and HELIAS (HELIcal-axis Advanced Stellarator) [3] 1 GW_e net electric output power plant.

Systems codes are a powerful tool for the rapid exploration of parameter space to obtain feasible and optimised designs. They work using simplified, yet comprehensive, models that cover the entire power plant, allowing the quick production of global designs; and one such code that is used extensively is PROCESS [4,5]. PROCESS takes a set of physics and engineering constraints, and solves for an optimised design based on a prescribed figure-of-merit. PROCESS has mostly been used to model conventional aspect ratio tokamaks and is used to produce the EUROfusion-DEMO baselines [6], however it also has the capabilities of modelling spherical tokamaks [7] and HELIAS-type stellarators [8,9].

In order to produce stellarator designs, three additional HELIAS specific models have been added to PROCESS [8,9]. Firstly, the plasma geometry is described using Fourier coefficients that can be obtained from a corresponding VMEC [10] equilibrium. This can be scaled, allowing for the determination of the cross-section and volume for any 3D shape. A basic island divertor model based on geometric considerations, assuming cross-field transport and X-point radiation, allows for the determination of the length of the divertor plate and heat load. Finally a modular coil model allows for the calculation of the maximum field at the coil, the total stored magnetic energy and the dimensions of the winding packs. In addition to these models, a number of stellarator specific confinement time scalings are implemented.

For each run PROCESS finds an optimal solution for a given set of inputs and constraints. However, this single solution does not account for the uncertainty on the design. In reality, individual inputs will have uncertainty based on extrapolation and modelling, and these uncertainties will interact with each other to produce the overall uncertainty on the design. To capture this, a Monte-Carlo based uncertainty tool has been developed for PROCESS that allows inputs to be defined by a distribution which represents a collection of uncertainties combined for that parameter. By performing the uncertainty analysis in a systems code, feasibility of integrated designs is preserved and the impact of multiple uncertainties can be evaluated at once. This technique has previously been applied to the EUROfusion-DEMO design [11–13], SST-2 [14] and

* Corresponding author.:
E-mail address: stuart.muldrew@ukaea.uk (S.I. Muldrew).

https://doi.org/10.1016/j.fusengdes.2021.112708
Received 7 July 2020; Received in revised form 21 May 2021; Accepted 28 May 2021
Available online 16 June 2021

CFETR [15]. In this paper we apply this technique to a stellarator design for the first time.

The rest of this paper is set out as follows: In Section 2 we describe the reference HELIAS 5-B design and the uncertainties that we have applied to it. In Section 3 we show the results of parameter studies and the Monte-Carlo based uncertainty analysis. We conclude in Section 4 by identifying the impact of our uncertainty analysis. Throughout this work we are using PROCESS version 1.0.15-45-g502bd05.

2. Design Uncertainties

The basis for our study is the HELIAS 5-B design presented by Warmer et al. [3]. Following that work, and revisions to PROCESS, we have made updates to the input leading to the baseline HELIAS 5-B PROCESS solution summarised in Table 1, and by the mean/peak values of Table 2. PROCESS has iterated on the density, temperature, β and bore size in order to maximise the net electric power output up to a maximum of 1 GW_e. The toroidal field, major radius and blanket thicknesses are given as input and no auxiliary heating is required to maintain fusion burn (i.e. the solution is ignited). The electrical power for cryogenics is 59 MW, using an efficiency of 13 per cent of ideal Carnot, while the pumping power for the primary coolant is the largest single use of recirculating power.

To quantify uncertainty on the HELIAS 5-B design, we used a Monte-Carlo based uncertainty tool with PROCESS. After identifying a set of input parameters to investigate, an uncertainty distribution was assigned to each one. Currently, Gaussian, upper and lower half-Gaussians and a uniform distribution are available. Gaussian distributions are defined by a mean and standard deviation, σ; while the upper and lower half-Gaussians are defined in the same way, however are truncated below or above the mean respectively. The uniform distribution is defined between a lower and upper bound. The Monte-Carlo code then draws at random from the distributions a value for each input and runs PROCESS to produce a solution. We repeat this 1,000 times to produce a range of output from which the overall uncertainty can be determined.

We have focused our uncertainty analysis on the reactor parameters and fixed the machine configuration. High impact design uncertainties can be considered as coming from two sources. Various constraints exist, such as on density or β, which limit the design space, however the exact value of these limits is unknown. The second source of design uncertainty is where an input parameter is simply not known to an adequate level of detail, for example the primary coolant pumping power. We identified eight parameters that potentially could have a high impact on the uncertainty of the HELIAS 5-B design. The uncertainty distributions assigned to them are listed in Table 2 and a brief description is found below. A detailed motivation of why each uncertainty was chosen will be presented in an upcoming paper by Warmer et al.

The eight uncertainties we identified were:

Primary coolant mechanical pumping power: The mechanical pumping power for the primary coolant required is dependent on the cooling technology and 200 MW was adopted for a Helium cooled HELIAS 5-B blanket [3]. While the expected pumping power is around this value [16] [6], other studies have shown values up to 400 MW [17]. This large range in pumping power can be attributed to uncertainty in the pressure drop [18], which requires a more detailed blanket design.

Core radius in radiation corrected confinement time scaling: Radiation from within the core radius is considered an instantaneous loss and is subtracted from the loss power for the confinement time scaling [19,20]. In this work we have fixed the fraction of radiation lost from within this radius to 100 per cent and only varied the size of the core radius. For the original HELIAS 5-B design a value of 0.9 was used [3], however, following more recent work [11], we have reduced it to 0.6 and centred our uncertainty distribution on that value.

Energy multiplication in the blanket: The energy multiplication is dependent on the blanket design and for HCPB (Helium Cooled Pebble Bed) this value can be high. In the previous HELIAS 5-B design a value of 1.18 was used [3], however more recent calculations suggest values as high as 1.35 could be achieved in advanced HCPB blankets for EUROfusion-DEMO [21]. The EUROfusion-DEMO baseline uses 1.269 for HCPB blankets [5] and a value of 1.27 is adopted here. This increase in energy multiplication will lead to a reduction in the fusion power relative to previous work.

Thermal He-4 number density fraction relative to n_e: While the production rate of helium ash is well understood, the fraction of thermal He-4 particles with respect to the electron density in the confined plasma is relatively uncertain, due to its dependence on particle transport, pumping in the main chamber and ELM (Edge Localised Mode) behaviour.

Tungsten number density fraction relative to n_e: Predicting the expected tungsten concentration is highly uncertain as it is unclear how much of the impurity will be screened, flushed outwards or drawn inwards [22]. Limits can, however, be imposed in order to make fusion burn possible, hence a mean of 10^{-5} was chosen [23]. The effect of the tungsten concentration on the HELIAS 5-B POPCON diagram is explored in [3].

βlimit: At increasing plasma pressure, the plasma becomes more stochastic at the edge essentially reducing the plasma volume. Increasing the pressure further will eventually lead to an MHD (Magneto-Hydro-Dynamic) stability limit. However, such a limit has so far not been experimentally observed.

Density limit: Stellarators do not have a hard density limit, unlike tokamaks with the Greenwald limit [24]. However, despite being ignited, it is advantageous to retain the capability to heat the plasma with ECRH (Electron Cyclotron Resonance Heating), therefore the density cannot be larger than the ECRH cut-off. This is determined by the magnetic field strength and associated ECRH frequency [25]. The density limit used is based on ITER-like 170 GHz gyrotrons, assuming a 10 per cent mirror term on the toroidal field, which accounts variation due to the configuration [26]. As the cut-off density is approached, the efficiency of the ECRH will drop due to deflection, therefore we have applied a safety margin of two-thirds of the limit.

Confinement renormalisation factor in relation to ISS04 [27] scaling: The confinement renormalisation factor is analogous to the H-factor for tokamaks, however it is motivated for different reasons. Clusters of data relating to different devices, and different magnetic configurations of the same device, are observed for stellarator confinement. Therefore, a configuration dependent parameter can be used to describe the improvement or degradation compared to the ISS04 [27] scaling. Transport codes can be used to predict the confinement time and hence the renormalisation factor. For a HELIAS 5-B configuration a minimum of 0.5, required for ignition, and a maximum of 1.5, from physics limits, were found [28]. We have chosen to adopt a flat distribution between the scaling relation and 1.5 to reflect this uncertainty.

3. Results

We have split our uncertainty analysis into two parts. Firstly we perform parameter studies on the individual uncertainties (Section 3.1) and then we combine the uncertainty distributions to perform Monte-Carlo based uncertainty analysis (Section 3.2).

3.1. Parameter Study

To begin we perform a parameter study for each uncertainty described in Section 2. Each uncertainty parameter was run in isolation 200 times using a value drawn from the distribution in Table 2. In Fig. 1 we plot histograms of the fusion power and give the convergence rate for each uncertainty parameter.

A PROCESS run is considered converged if a feasible solution, obeying the constraints set for the given input parameters, is found. Conversely, unconverged solutions are when PROCESS cannot find a feasible solution

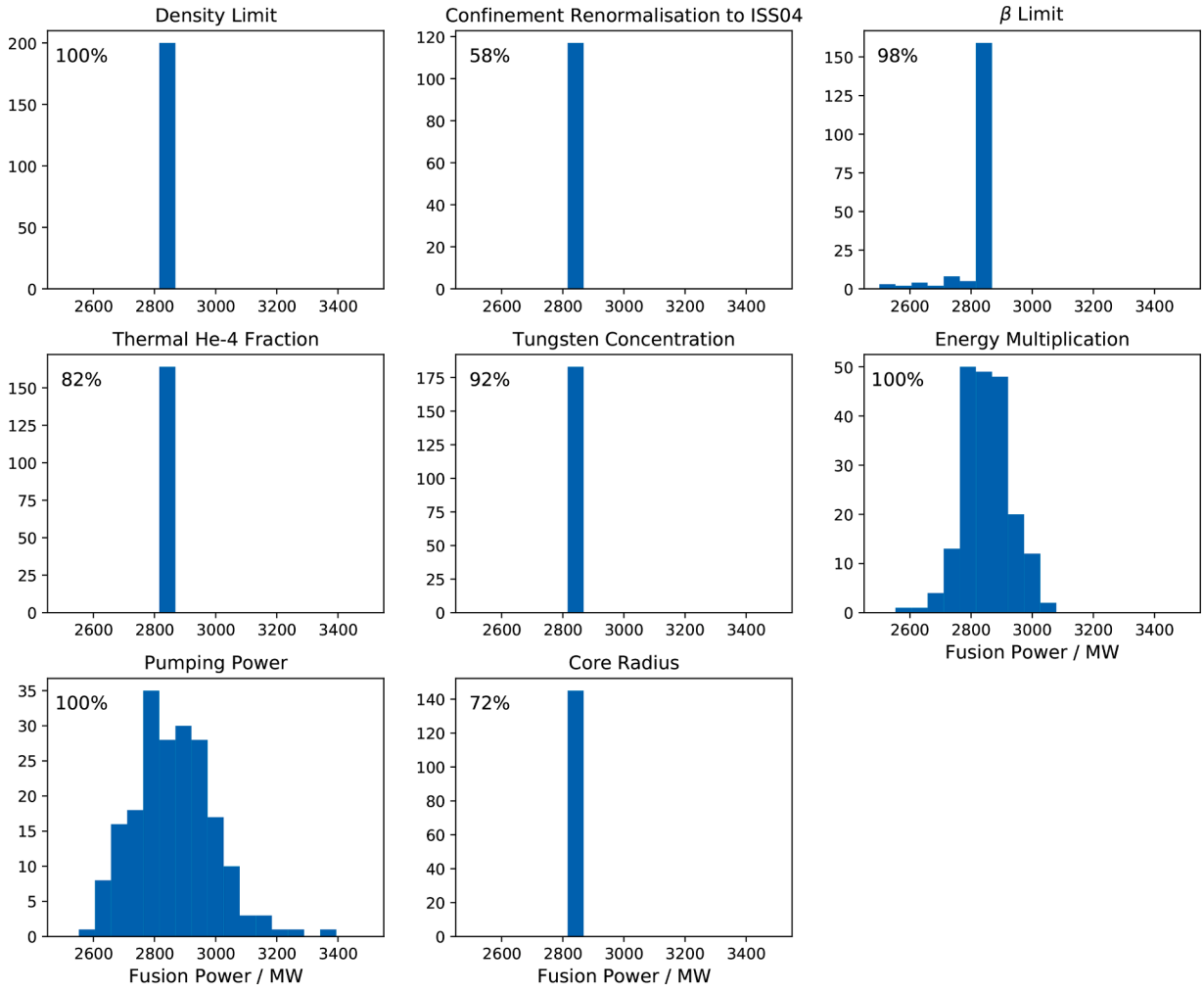

Fig. 1. The distribution of fusion power for each input uncertainty. For each graph PROCESS has been run 200 times varying only the uncertainty described in the title. The *x*-axis gives the fusion power in MW, the *y*-axis gives the frequency and the percentage in the top left corner of each graph corresponds to the fraction of runs that converged.

for the input. The convergence rate is then defined as the fraction of feasible solutions found out of the total runs conducted, and only these are considered for analysis. The convergence rate is generally high, with the confinement renormaliation and core radius having the biggest impact on convergence. The cause of this will become more apparent in Section 3.2. The thermal He-4 fraction also has an effect on the convergence.

Throughout this work we optimised for maximum net electricity up to 1 GW_e. In terms of the fusion power, only three uncertainties have an impact. The largest spread of fusion power comes from the primary coolant pumping power, followed by the energy multiplication. These are expected to be high impact as they directly affect the net electricity output and hence the fusion power required. For higher pumping powers, a higher gross electric output is required to maintain the same net output. This is achieved by raising the fusion power. It should be noted that the electrical power for the pumps is transferred to mechanical power in the coolant, and so also contributes to the thermal power, hence this is not simply a one-to-one relation. For the energy multiplication, a higher multiplication in the blanket requires a lower fusion power to give the same thermal power. The final uncertainty to influence the fusion power is the β limit. This has a smaller effect because the majority of solutions are not constrained by the β limit.

3.2. Monte-Carlo Uncertainty

We now move on to the Monte-Carlo uncertainty analysis. As described in Section 2, a value for each input being studied was drawn at random from the uncertainty distributions in Table 2, and then combined to form a PROCESS input. A total of 1,000 different combinations of these values were generated and run. The input values used are shown by the blue histograms in Fig. 2.

For each input distribution we also plot the distribution of converged solutions as orange histograms in Fig. 2. This will illustrate areas of parameter space where there are no viable solutions. For the majority of parameters, the recovered distribution is similar to the input distribution, however this is not the case for the confinement renormalisation factor with respect to ISS04. This also had the lowest convergence rate in Fig. 1. A uniform input distribution between 1.0 and 1.5 was given, however below 1.2 the number of converged solutions is significantly reduced. Above 1.2 the flat distribution is still recovered.

The cause of this reduction is shown in the left panel of Fig. 3 which gives the volume averaged density, temperature and confinement renomalisation factor for the converged solutions. 1D parametric density and temperature profiles are used within the code, with the same parameters used in all runs. The ratio of the ion to electron temperature is 0.95. Fig. 3 should be compared with the top left panel of Fig. 2, which gives the density limit imposed based on the ECRH cut-off. As the density increases, the required renormalisation factor to achieve the fusion

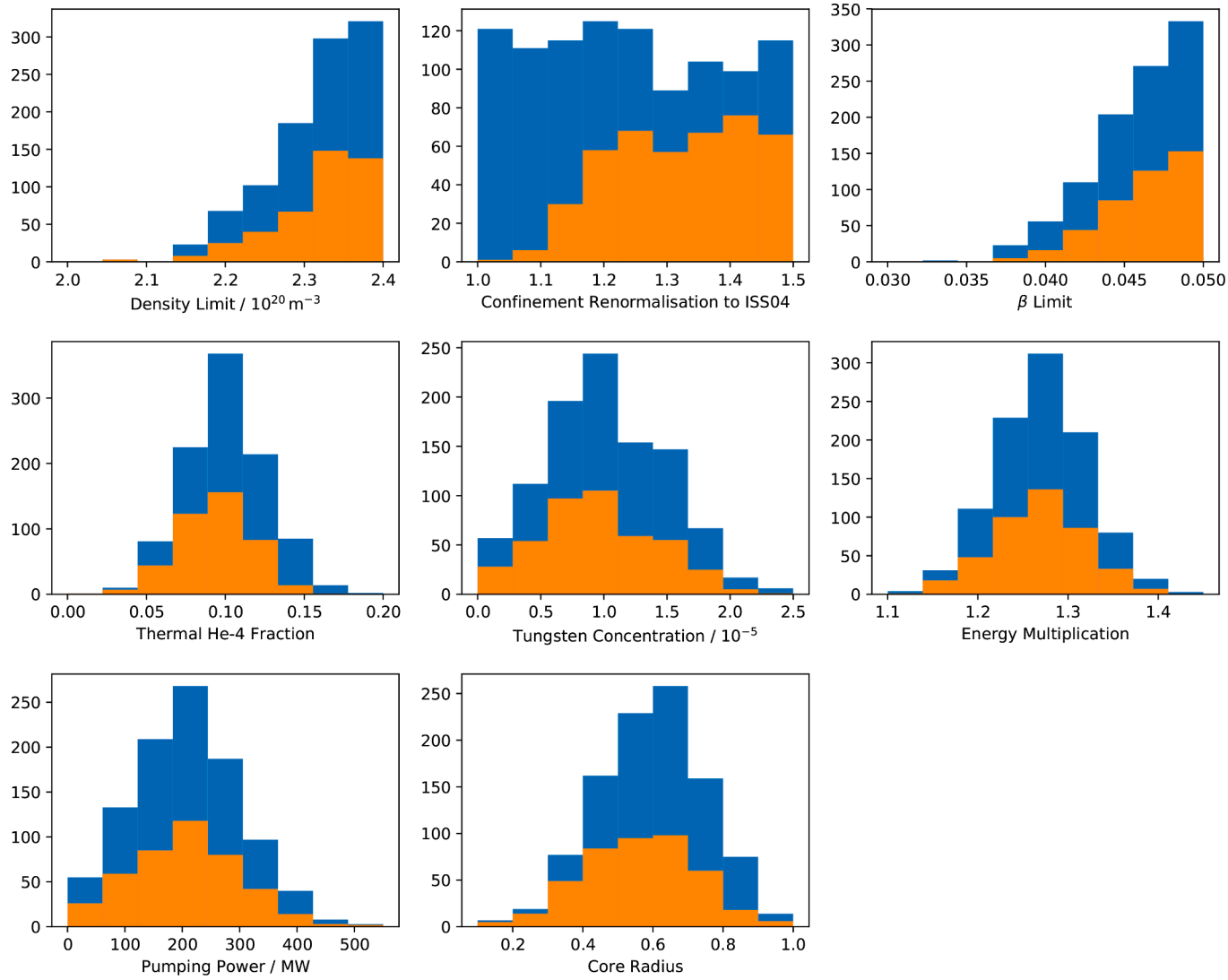

Fig. 2. The uncertainty distributions summarised in Table 2 and those recovered from the converged runs. Blue histograms are the input values, while orange represents the distribution of converged solutions. The *x*-axis gives values of the uncertainty and the *y*-axis gives the frequency. The confinement renormalisation factor (top middle) is the most noticeably different with low values of f_{ren} not converging.

power decreases. As the density is limited, it is not possible to access the higher values that will lead to a lower normalisation factor, hence no converged solutions can be found.

The remaining two panels of Fig. 3 illustrate the dependence on β and the fusion power. For a fixed density, higher β is associated with higher temperatures. The final panel illustrates a number of different combinations possible to produce the required fusion power. Overall, there is a clear density and temperature trend that is related to the required confinement renormalisation, and hence the confinement time scaling law used. Scatter is then induced by different values of β.

Of the 1,000 PROCESS runs we performed for the Monte-Carlo based analysis, 429 converged on a solution. Of those converged solutions, 73 per cent achieved the required 1 GW_e of net electric output. The mean fusion power for 1 GW_e of net electric output is 2,852 MW with a standard deviation of 131 MW. If all the converged solutions are considered, with the lower net electric out, then this becomes a mean of 2,786 MW and a standard deviation of 199 MW.

From Fig. 1 we have identified that the primary coolant mechanical pumping power and blanket energy multiplication have the strongest influence on the required fusion power to produce 1 GW_e of net electricity. We now explore these in more detail.

In Fig. 4 we plot the primary coolant mechanical pumping power against the fusion power, colour coded by the net electric output. Considering the 1 GW_e net electric cases, a strong linear correlation is seen between increasing pumping power and increasing fusion power. Taking the gradient of this relation yields a value of a 1.26 MW increase in fusion power for every 1 MW of pumping power. As the pumping power is increased, the only solution is to increase the fusion power in order to cover the increase in gross electric, to maintain the same net electric output. It can also be seen from Fig. 4 that the primary pumping power is not the only source of uncertainty. Even for a fixed pumping power, there is still a scatter of 200 MW in the required fusion power.

We have adopted a very broad Gaussian for the pumping power that stretches down to 0 MW to fully illustrate the impact. Low values would be hard to achieve with Helium, however other coolant choices could decrease the pumping requirements. The gap that opens up below the main sequence, for low pumping powers, is indicative of the fact it is easier to achieve 1 GW_e of net electric with lower pumping power.

In Fig. 5 we address the second most influential input from the parameter study in Section 3.1, the blanket energy multiplication. The trend of decreasing fusion power, with increasing energy multiplication, is observed as expected. The scatter however is very broad, indicating a lesser dependence on this parameter. The level of scatter can be quantified by performing a least-squares linear fit to the 1 GW_e points and

Table 1
Reference values for HELIAS 5-B to three significant figures. The density and temperature are volume-averaged.

Parameter	Ref
Major Radius, R_0 (m)	22.0
Minor Radius, a (m)	1.80
Plasma Cross-Sectional Area (m^2)	10.2
Plasma Volume (m^3)	1410
HELIAS Field Periods	5
Number of Coils	50
Superconducting Material	Nb_3Sn
Thermal efficiency, η_{th}	0.4
Toroidal Field, B_t (T)	5.50
Volume-averaged β (%)	4.36
Rotational Transform at $\rho = 2/3$, $\iota/2\pi$	0.900
Divertor Heat Load ($MW\,m^{-2}$)	3.99
Electron Density, $\langle n_e \rangle$ ($10^{20}\,m^{-3}$)	1.91
Electron Temperature, $\langle T_e \rangle$ (keV)	7.45
Confinement Renormalisation Factor, f_{ren}	1.25
Fusion Power, P_{fus} (MW)	2850
Net Electric Power, P_{net} (MW)	1000

Table 2
Uncertainty distributions applied to the HELIAS 5-B PROCESS input, see the bold text in Section 2 for an explanation. σ is the standard deviation used in the Gaussian and the distributions are visualised by the blue histograms in Fig. 2.

Gaussian	**Mean**	σ
Coolant Pumping Power (MW)	200	100
Core Radius	0.60	0.15
Energy Multiplication	1.27	0.05
Thermal He-4 Fraction	0.100	0.025
Tungsten Density Fraction (10^{-5})	1.0	0.5
Lower-Half Gaussian	**Peak**	σ
β Upper Limit (%)	5.00	0.50
Density Upper Limit ($10^{20}\,m^{-3}$)	2.4	0.1
Uniform	**Lower**	**Upper**
Confinement Renormalisation	1.0	1.5

computing the Coefficient of Determination, R^2. R^2 is defined as the proportion of the variance in the dependent variable that is predictable from the independent variable. Higher values indicate a tighter fit with $R^2 = 1$ being a perfect fit. For the blanket energy multiplication $R^2 = 0.24$, compared with a value of $R^2 = 0.71$ for the mechanical pumping power. Overall, the uncertainty in these two parameters covers the majority of the uncertainty induced by the inputs studied here. This indicates that research on the blankets should be prioritised to reduce uncertainty on the overall design.

The impact of a different fusion power will be felt in the heat load on the divertor, and this is illustrated in Fig. 6. The peak steady-state tolerable heat load is taken as $5\,MW\,m^{-2}$, similar to that of EUROfusion-DEMO [29], and the region above this is shaded grey in the figure. As well as the fusion power, the divertor heat load will also be affected by the level of tungsten impurity. For a higher level of impurity, more power will be radiated from the core plasma and not end up on the divertor. To illustrate this we have colour coded the points in Fig. 6. For all the converged cases, 83 per cent of solutions are below $5\,MW\,m^{-2}$; this reduces to 81 per cent if only the solutions producing 1 GW_e of net electricity are considered. The mean heat load on the divertor is $4.33\,MW\,m^{-2}$ with a standard deviation of $0.82\,MW\,m^{-2}$ for all cases. This becomes a mean of $4.48\,MW\,m^{-2}$ and standard deviation of $0.64\,MW\,m^{-2}$ when limited to those producing 1 GW_e of net electricity. An extreme outlier is shown with close to zero divertor heat load, which will be caused by a high radiative fractions indicated by the high tungsten concentration. This would most likely be unfeasible and an additional constrain should be added in future runs.

4. Conclusions

In this paper we have explored the uncertainty on a HELIAS 5-B stellarator power plant design using PROCESS. The design uncertainties identified include the primary coolant mechanical pumping power, the core radius in the radiation corrected confinement time scaling, the

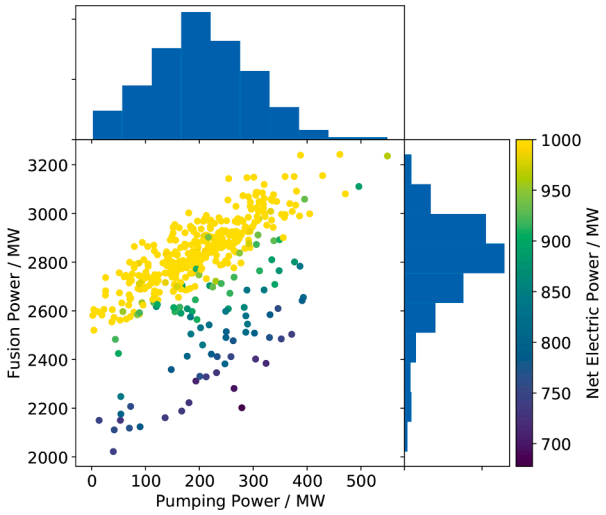

Fig. 4. The input primary coolant mechanical pumping power plotted against the required fusion power. Runs have been performed maximising the net electric output up to 1 GW_e, and this is illustrated by the colour bar.

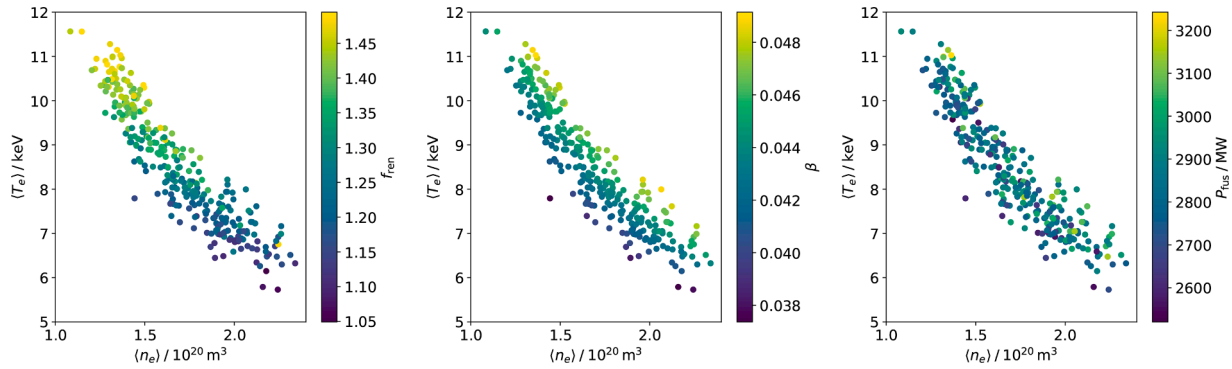

Fig. 3. The volume averaged electron temperature against the volume averaged electron density, colour coded by renormalisation factor in relation to ISS04 (left), total β (middle) and fusion power (right).

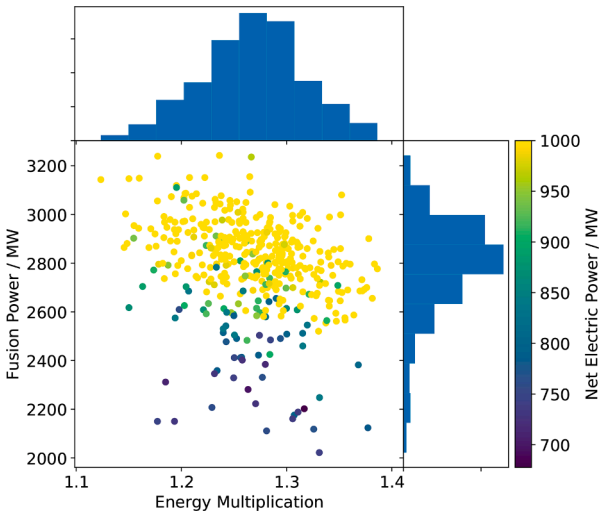

Fig. 5. The blanket energy multiplication plotted against the required fusion power. Runs have been performed maximising the net electric output up to 1 GW_e, and this is illustrated by the colour bar.

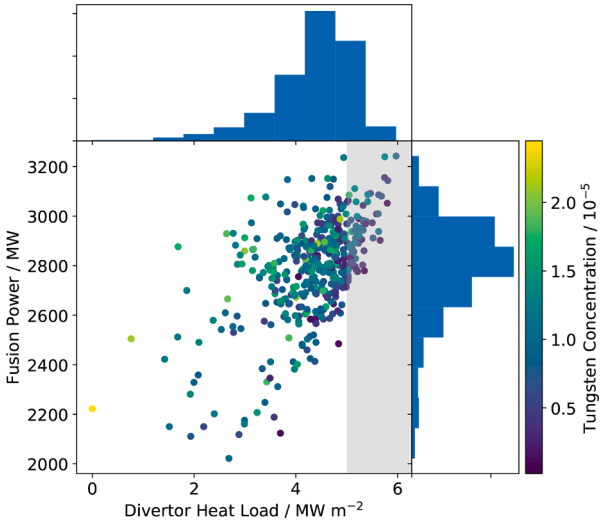

Fig. 6. The heat load on the divertor plotted against the required fusion power. Runs have been performed maximising the net electric output up to 1 GW_e. The colour bar illustrates the level of tungsten concentration, while the shaded grey region shows solutions above the tolerable 5 MW m^{-2}.

energy multiplication in the blanket and shield, the thermal He-4 number density, the tungsten number density, the β limit, the density limit and the confinement renormalisation in relation to ISS04.

We found that the required renormalisation on the confinement time relative to ISS04 is impacted by the density limit for ECRH. For low renormalisation factors, the density required is above the density limit and so no feasible solutions for a 1 GW_e net electric power plant are found. This relates back to the strong density dependence in the ISS04 scaling, $\tau_E \propto \bar{n}^{0.54}$, which means higher density gives better confinement without renormalisation. Whether this holds for highly radiative plasmas is unclear (see [30]), and this emphasises the need to understand confinement in stellarator power plants.

For the uncertainties studied here, we found the two that have the strongest influence on the fusion power are the mechanical pumping power and blanket energy multiplication. The variation in these leads to a 131 MW standard deviation in the fusion power of 1 GW_e net electric producing plants. This shows that the blankets should be prioritised for research to reduce overall design uncertainty. 83 per cent of these runs, however, remain below the 5 MW m^{-2} that is tolerable on the divertor. The divertor protection is also impacted by the tungsten impurity concentration in the plasma, which is another key uncertainty to understand the design.

Overall, the uncertainties studied here are the ones we have identified specific to the reactor. There are other elements of the power plant that will also lead to variations. Most importantly of these is the thermal-to-electric conversion efficiency which we have not varied from 0.4. This is highly dependent on the temperature of the thermal cycle and the technology used. Small variations in the percentage can lead to large variations in the fusion power; for example a variation of 5 per cent on the efficiency can raise or lower the net electric out by 174 MW. It is vitally important that this technology is understood for all fusion power plants and more detailed blanket and thermal cycle designs are needed for this.

We have restricted our analysis in this work to a HELIAS 5-B stellarator as PROCESS is currently only capable of modelling stellarators of this type. We are, however, extending the code to model a broader class of stellarators [31], with one such example being the new quasi-axisymmetric configuration [32]. This will allow us to compare and contrast the designs, as well as bound the impact of uncertainties in each, to propose the optimal stellarator fusion power plant.

Disclosure of conflicts of interest

The authors declare that they have no known competing financial interests or personal relationships that could have appeared to influence the work reported in this paper.

CRediT authorship contribution statement

Stuart I. Muldrew: Conceptualization, Methodology, Software, Formal analysis, Investigation, Writing - original draft, Writing - review & editing, Visualization. **Felix Warmer:** Conceptualization, Methodology, Software, Validation, Project administration, Funding acquisition. **Jorrit Lion:** Methodology, Software, Writing - review & editing. **Hanni Lux:** Methodology, Supervision, Funding acquisition.

Declaration of Competing Interest

The authors declare that they have no known competing financial interests or personal relationships that could have appeared to influence the work reported in this paper.

Acknowledgements

This work has been carried out within the framework of the EUROfusion Consortium and has received funding from the Euratom research and training programme 2014-2018 and 2019-2020 under grant agreement No 633053 and from the RCUK [grant number EP/T012250/1]. To obtain further information on the data and models underlying this paper please contact PublicationsManager@ukaea.uk. The views and opinions expressed herein do not necessarily reflect those of the European Commission.

Supplementary material

Supplementary material associated with this article can be found, in the online version, at 10.1016/j.fusengdes.2021.112708

References

[1] A.J.H. Donné, A.W. Morris, European research roadmap to the realisation of fusion energy, EUROfusion (2018) (2018).http://www.euro-fusion.org/eurofusion/roadmap

[2] T. Goto, J. Miyazawa, H. Tamura, T. Tanaka, S. Hamaguchi, N. Yanagi, A. Sagara, t. F.D. Group, Design window analysis for the helical DEMO reactor FFHR-d1, Plasma

and Fusion Research 7 (2012) 2405084, https://doi.org/10.1585/pfr.7.2405084. https://www.jstage.jst.go.jp/article/pfr/7/0/7_2405084/_article

[3] F. Warmer, S.B. Torrisi, C.D. Beidler, A. Dinklage, Y. Feng, J. Geiger, F. Schauer, Y. Turkin, R. Wolf, P. Xanthopoulos, R. Kemp, P. Knight, H. Lux, D. Ward, System code analysis of HELIAS-type fusion reactor and economic comparison with tokamaks, IEEE Transactions on Plasma Science 44 (9) (2016) 1576–1585, https://doi.org/10.1109/TPS.2016.2545868.https://ieeexplore.ieee.org/abstract/document/7448445

[4] M. Kovari, R. Kemp, H. Lux, P. Knight, J. Morris, D.J. Ward, "PROCESS": A systems code for fusion power plants – Part 1: Physics, Fusion Engineering and Design 89 (12) (2014) 3054–3069, https://doi.org/10.1016/j.fusengdes.2014.09.018.http://www.sciencedirect.com/science/article/pii/S0920379614005961

[5] M. Kovari, F. Fox, C. Harrington, R. Kembleton, P. Knight, H. Lux, J. Morris, "PROCESS": A systems code for fusion power plants – Part 2: Engineering, Fusion Engineering and Design 104 (2016) 9–20, https://doi.org/10.1016/j.fusengdes.2016.01.007.http://www.sciencedirect.com/science/article/pii/S0920379616300072

[6] R. Wenninger, R. Kembleton, C. Bachmann, W. Biel, T. Bolzonella, S. Ciattaglia, F. Cismondi, M. Coleman, A.J.H. Donné, T. Eich, E. Fable, G. Federici, T. Franke, H. Lux, F. Maviglia, B. Meszaros, T. Pütterich, S. Saarelma, A. Snickers, F. Villone, P. Vincenzi, D. Wolff, H. Zohm, The physics and technology basis entering European system code studies for DEMO, Nuclear Fusion 57 (1) (2017) 016011.http://stacks.iop.org/0029-5515/57/i=1/a=016011

[7] S.I. Muldrew, H. Lux, G. Cunningham, T.C. Hender, S. Kahn, P.J. Knight, B. Patel, G.M. Voss, H.R. Wilson, "PROCESS": Systems studies of spherical tokamaks, Fusion Engineering and Design 154 (2020) 111530, https://doi.org/10.1016/j.fusengdes.2020.111530.http://www.sciencedirect.com/science/article/pii/S0920379620300788

[8] F. Warmer, C.D. Beidler, A. Dinklage, K. Egorov, Y. Feng, J. Geiger, F. Schauer, Y. Turkin, R. Wolf, P. Xanthopoulos, HELIAS module development for systems codes, Fusion Engineering and Design 91 (2015) 60–66, https://doi.org/10.1016/j.fusengdes.2014.12.028.http://www.sciencedirect.com/science/article/pii/S0920379614006723

[9] F. Warmer, C.D. Beidler, A. Dinklage, K. Egorov, Y. Feng, J. Geiger, R. Kemp, P. Knight, F. Schauer, Y. Turkin, D. Ward, R. Wolf, P. Xanthopoulos, Implementation and verification of a HELIAS module for the systems code PROCESS, Fusion Engineering and Design 98-99 (2015) 2227–2230, https://doi.org/10.1016/j.fusengdes.2014.12.021.http://www.sciencedirect.com/science/article/pii/S0920379614006656

[10] S.P. Hirshman, W.I. van Rij, P. Merkel, Three-dimensional free boundary calculations using a spectral Green's function method, Computer Physics Communications 43 (1) (1986) 143–155, https://doi.org/10.1016/0010-4655(86)90058-5.http://www.sciencedirect.com/science/article/pii/0010465586900585

[11] H. Lux, R. Kemp, R. Wenninger, W. Biel, G. Federici, W. Morris, H. Zohm, Uncertainties in power plant design point evaluations, Fusion Engineering and Design 123 (2017) 63–66, https://doi.org/10.1016/j.fusengdes.2017.01.029. http://www.sciencedirect.com/science/article/pii/S092037961730039X

[12] R. Kemp, H. Lux, M. Kovari, J. Morris, R. Wenninger, H. Zohm, W. Biel, G. Federici, Dealing with uncertainties in fusion power plant conceptual development, Nuclear Fusion 57 (4) (2017) 046024, https://doi.org/10.1088/1741-4326/aa5e2c.

[13] H. Lux, M. Siccinio, W. Biel, G. Federici, R. Kembleton, A.W. Morris, E. Patelli, H. Zohm, Implications of uncertainties on European DEMO design, Nuclear Fusion 59 (6) (2019) 066012, https://doi.org/10.1088/1741-4326/ab13e2.

[14] S.I. Muldrew, H. Lux, V. Menon, R. Srinivasan, Uncertainty analysis of an SST-2 fusion reactor design, Fusion Engineering and Design 146 (2019) 353–356, https://doi.org/10.1016/j.fusengdes.2018.12.066.http://www.sciencedirect.com/science/article/pii/S0920379618308317

[15] J. Morris, V. Chan, J. Chen, S. Mao, M.Y. Ye, Validation and sensitivity of CFETR design using EU systems codes, Fusion Engineering and Design 146 (2019) 574–577, https://doi.org/10.1016/j.fusengdes.2019.01.026.http://www.sciencedirect.com/science/article/pii/S0920379619300341

[16] A.R. Raffray, L. El-Guebaly, S. Malang, X.R. Wang, L. Bromberg, T. Ihli, B. Merrill, L. Waganer, A.-C. Team, Engineering design and analysis of the ARIES-CS power plant, Fusion Science and Technology 54 (3) (2008) 725–746, https://doi.org/10.13182/FST08-4.

[17] D. Maisonnier, D. Campbell, I. Cook, L.D. Pace, L. Giancarli, J. Hayward, A. L. Puma, M. Medrano, P. Norajitra, M. Roccella, P. Sardain, M.Q. Tran, D. Ward, Power plant conceptual studies in Europe, Nuclear Fusion 47 (11) (2007) 1524–1532, https://doi.org/10.1088/0029-5515/47/11/014.

[18] F. Warmer, E. Bubelis, First considerations on the Balance of Plant for a HELIAS fusion power plant, Fusion Engineering and Design 146 (2019) 2259–2263, https://doi.org/10.1016/j.fusengdes.2019.03.167.http://www.sciencedirect.com/science/article/pii/S0920379619305022

[19] H. Lux, R. Kemp, D.J. Ward, M. Sertoli, Impurity radiation in DEMO systems modelling, Fusion Engineering and Design 101 (2015) 42–51, https://doi.org/10.1016/j.fusengdes.2015.10.002.http://www.sciencedirect.com/science/article/pii/S0920379615302891

[20] H. Lux, R. Kemp, E. Fable, R. Wenninger, Radiation and confinement in 0D fusion systems codes, Plasma Physics and Controlled Fusion 58 (7) (2016) 075001, https://doi.org/10.1088/0741-3335/58/7/075001.

[21] P. Pereslavtsev, U. Fischer, F. Hernandez, L. Lu, Neutronic analyses for the optimization of the advanced HCPB breeder blanket design for DEMO, Fusion Engineering and Design 124 (2017) 910–914, https://doi.org/10.1016/j.fusengdes.2017.01.028.http://www.sciencedirect.com/science/article/pii/S0920379617300388

[22] R. Dux, A. Loarte, E. Fable, A. Kukushkin, Transport of tungsten in the H-mode edge transport barrier of ITER, Plasma Physics and Controlled Fusion 56 (12) (2014) 124003, https://doi.org/10.1088/0741-3335/56/12/124003.

[23] T. Pütterich, R. Neu, R. Dux, A.D. Whiteford, M.G. O'Mullane, H.P. Summers, A. U. Team, Calculation and experimental test of the cooling factor of tungsten, Nuclear Fusion 50 (2) (2010) 025012, https://doi.org/10.1088/0029-5515/50/2/025012.

[24] M. Greenwald, J.L. Terry, S.M. Wolfe, S. Ejima, M.G. Bell, S.M. Kaye, G.H. Neilson, A new look at density limits in tokamaks, Nuclear Fusion 28 (12) (1988) 2199. http://stacks.iop.org/0029-5515/28/i=12/a=009

[25] V. Erckmann, U. Gasparino, Electron cyclotron resonance heating and current drive in toroidal fusion plasmas, Plasma Physics and Controlled Fusion 36 (12) (1994) 1869–1962, https://doi.org/10.1088/0741-3335/36/12/001.

[26] F. Warmer, C.D. Beidler, A. Dinklage, R.W. and, From W7-X to a HELIAS fusion power plant: motivation and options for an intermediate-step burning-plasma stellarator, Plasma Physics and Controlled Fusion 58 (7) (2016) 074006, https://doi.org/10.1088/0741-3335/58/7/074006.

[27] H. Yamada, J.H. Harris, A. Dinklage, E. Ascasibar, F. Sano, S. Okamura, J. Talmadge, U. Stroth, A. Kus, S. Murakami, M. Yokoyama, C.D. Beidler, V. Tribaldos, K.Y. Watanabe, Y. Suzuki, Characterization of energy confinement in net-current free plasmas using the extended International Stellarator Database, Nuclear Fusion 45 (12) (2005) 1684–1693, https://doi.org/10.1088/0029-5515/45/12/024.

[28] F. Warmer, C.D. Beidler, A. Dinklage, Y. Turkin, R. Wolf, Limits of confinement enhancement for stellarators, Fusion Science and Technology 68 (4) (2015) 727–740, https://doi.org/10.13182/FST15-131.

[29] H. Reimerdes, R. Ambrosino, P. Innocente, A. Castaldo, P. Chmielewski, G. D. Gironimo, S. Merriman, V. Pericoli-Ridolfini, L. Aho-Mantilla, R. Albanese, H. Bufferand, G. Calabro, G. Ciraolo, D. Coster, N. Fedorczak, S. Ha, R. Kembleton, K. Lackner, V.P. Loschiavo, T. Lunt, D. Marzullo, R. Maurizio, F. Militello, G. Ramogida, F. Subba, S. Varoutis, R. Zagórski, H. Zohm, Assessment of alternative divertor configurations as an exhaust solution for DEMO, Nuclear Fusion 60 (6) (2020) 066030, https://doi.org/10.1088/1741-4326/ab8a6a.

[30] G. Fuchert, K.J. Brunner, K. Rahbarnia, T. Stange, D. Zhang, J. Baldzuhn, S. A. Bozhenkov, C.D. Beidler, M.N.A. Beurskens, S. Brezinsek, R. Burhenn, H. Damm, A. Dinklage, Y. Feng, P. Hacker, M. Hirsch, Y. Kazakov, J. Knauer, A. Langenberg, H.P. Laqua, S. Lazerson, N.A. Pablant, E. Pasch, F. Reimold, T.S. Pedersen, E. R. Scott, F. Warmer, V.R. Winters, R.C. Wolf, W.-X. Team, Increasing the density in Wendelstein 7-X: benefits and limitations, Nuclear Fusion 60 (3) (2020) 036020, https://doi.org/10.1088/1741-4326/ab6d40.

[31] J. Lion, F. Warmer, C.D. Beidler, R.C. Wolf, Towards generalized systems code models for arbitrary modular stellarators, (22nd International Stellarator and Heliotron Workshop (21-25 September 2019); Madison, WI, USA).

[32] S.A. Henneberg, M. Drevlak, C. Nührenberg, C.D. Beidler, Y. Turkin, J. Loizu, P. Helander, Properties of a new quasi-axisymmetric configuration, Nuclear Fusion 59 (2) (2019) 026014, https://doi.org/10.1088/1741-4326/aaf604.